Flow of Liquid Jets through Closely Woven Screens

Franklin T. Dodge* and Randall E. Ricker†
Southwest Research Institute, San Antonio, Texas

Previously developed analytical models relate pressure drop across a fine-mesh screen to throughflow velocity for duct systems. These models are shown to be unreliable for an unconfined flow, such as a free jet, impinging on a screen. A new model is developed for these kinds of systems, incorporating the important influence of liquid deflection by the screen. A new parameter, the boundary-layer blockage coefficient, is introduced. This coefficient, which depends on the screen weave geometry and the jet impingement angle, accounts for the increase in fluid path length through the screen resulting from the flow deflection. Comparisons are made with previous experimental studies to determine empirical values of the blockage coefficient. It is concluded that the new model reliably predicts the bulk flow and penetration characteristics of an impinging liquid jet interacting with a screen.

Nomenclature

a = surface area to unit volume ratio of screen, cm^{-1}
A = screen geometrical constant, $\alpha a^2 bQ/E^2$, cm^{-1}
b = thickness of screen, cm
B = screen geometrical constant, $\beta bQ/E^2 D$
C_p = pressure coefficient
D = screen pore diameter, cm
ΔP = pressure drop across screen, N/cm^2
Q = tortuosity factor
r,θ,z = coordinate system centered at jet stagnation point; r, θ in plane of screen, z positive upward
R_j = impinging jet radius, cm
V = throughflow velocity, cm/s
V_{av} = average throughflow velocity, cm/s
V_j = impinging jet velocity, cm/s
V_s = boundary-layer slip velocity, cm/s
x = r/R_j
α = viscous resistance coefficient
β = inertial resistance coefficient
ϵ = screen-volume void fraction
μ = liquid viscosity, g/cm-s
ϕ = blockage coefficient
π_1 = dimensionless parameter, $A\mu/\rho V_j$
π_2 = dimensionless parameter, π_1^2/B
π_3 = dimensionless parameter, $0.074\,(\rho b^2 V_j/\mu R_j)^{1/2}\,\pi_1$
ρ = liquid density, g/cm^3

Introduction

RECENT studies have shown that fine-mesh screens make an excellent system for controlling liquids in spacecraft propellant tanks during periods of reduced gravity. Typical applications are providing vapor-free liquid for restarting an engine and for transfer from one storage tank to another. To be successful, the devices must be capable of being refilled after use. Although such basic screen characteristics as wicking and flowthrough pressure drop have been studied at length, little effort has been spent on understanding liquid behavior during refilling. In particular, work has just started on the study of impingement of an unconfined flow upon a screen, which is a likely refilling procedure.

Received Nov. 21, 1977; revision received March 3, 1978.

Index categories: Jets, Wakes, and Viscid-Inviscid Flow Interactions; Liquid Rocket Engines and Missile Systems.

*Staff Engineer, Department of Mechanical Sciences. Associate Fellow AIAA.

†Engineer, Department of Mechanical Sciences. Member AIAA.

Several correlations have been developed (Refs. 1-5, for example) to relate the throughflow velocity V and pressure drop ΔP across a screen. Most are of the form originated by Armour and Cannon[1]:

$$\Delta P = \alpha(a^2 bQ/\epsilon^2)\mu V + \beta(bQ/\epsilon^2 D)\rho V^2 \qquad (1)$$

Both α and β are empirical factors that represent, respectively, viscous and inertial contributions to ΔP. The other factors in Eq. (1) are geometric properties of the weave and physical properties of the liquid. Armour and Cannon's tests gave universal factors of 8.61 for α and 0.52 for β. More recent tests (Refs. 2 and 3, for example) indicate that these parameters depend upon the screen weave. All of these correlations apply to flow confined by the walls of a tube, across a perpendicularly oriented screen, and thus are unlikely to be useful for predicting throughflow of a free jet or unconfined flow impinging upon a screen. Impingement tests of a circular jet[4] have shown, in fact, that Eq. (1) can over-

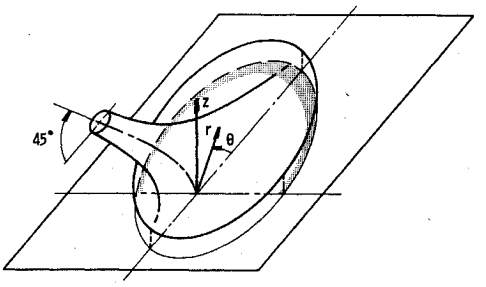

a) 45-deg oblique impingement of a circular jet

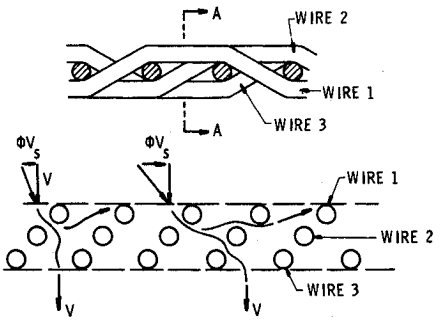

b) Boundary-layer blockage (twilled Dutch)

Fig. 1 Geometry of jet-screen impingement model.

predict the throughflow by 100%, a conclusion arrived at by interpreting ΔP as the average pressure (i.e., the impact force of the jet divided by the impact area) on the upstream screen surface. Much of the liquid was simply deflected as if by a baffle.

The analysis presented here was undertaken to help gain an understanding of the impingement of a liquid jet on a screen. Computer or wholly numerical models have been excluded, to emphasize physical understanding and to enable the model to be used economically for design and parametric studies. Two cases were studied: normal impingement, and oblique impingement at 45 deg.

Modeling of Screen Throughflow

Modeling Approach

Analysis of jet flow through a screen, as shown in Fig. 1, requires knowledge of the driving pressure distribution at all points on the screen; thus, the first modeling task is to derive expressions for the pressures. Next, a physical model of the flow within and through the screen is proposed, using Eq. (1) as a starting point; the formulation of this flow model constitutes the main original effort of the analysis.

Impingement Pressure

A previous theory[6] predicts both pressure and tangential velocity for normal impingement of a circular jet on an impermeable plane; these predictions were also verified by us by an independent numerical computation.‡ These show that the pressure and tangential (radial) velocity results can be closely correlated by

$$\Delta P = \tfrac{1}{2}\rho C_p V_j^2 \qquad C_P = 1 - 0.25(r/R_j)^2 \tag{2}$$

and

$$V_r = 0.5 V_j (r/R_j) \tag{3}$$

Positive ΔP implies that liquid will flow through the screen; thus, since $C_p \geq 0$ for $r \leq 2R_j$, Eq. (3) indirectly verifies one of the conclusions of Ref. 4, namely, that the emerging jet has a diameter about twice that of the impinging jet.

Previous models of oblique impingement apply only to two-dimensional or rectangular jets (Refs. 6 and 7, for example). Numerical solutions, even for one angle of obliquity, were impractical for this study. Consequently, an approximate procedure is used to predict the pressure distribution. Details are given in Ref. 8. The analytical expressions are

$$C_p = 1 - 0.25(r/R_j)^2 \qquad (-90 \leq \theta \leq 90 \text{ deg}) \tag{4a}$$

$$C_p = [1 - (r/R_j)^2]\cos^2\theta + [1 - 0.25(r/R_j)^2]\sin^2\theta \qquad (90 \leq \theta \leq 270 \text{ deg}) \tag{4b}$$

$$V_r = 0.5 V_j [r/(1 + \tfrac{1}{2}\cos\theta) R_j] \tag{5}$$

The coordinate system is shown in Fig. 1a. Equation (4a) neglects a region of small pressure shown by the shaded area in this figure. Also, in Eq. (4b) r must be limited to values less than R_j for the term multiplied by $\cos^2\theta$. The total force, $\pi\rho V^2 R^2 \cos 45$, is overpredicted by Eqs. (4a) and (4b) but by less than 15%.

Predictions of Unmodified Model

The applicability of Eq. (1) can be determined by substituting into it Eq. (2), for normal impingement, or Eqs. (4a) and (4b), for 45-deg impingement. The solution for V is

$$V = \frac{A\mu}{2B\rho}\left[\sqrt{1 + \frac{2C_p V_j^2}{B}\left(\frac{\rho B}{\mu A}\right)^2} - 1\right] \tag{6}$$

where $A = \alpha(a^2 bQ/\epsilon^2)$ and $B = \beta(bQ/D\epsilon^2)$. Equation (6) gives the velocity of the emergent jet as a function of r and θ, since C_P depends on r and θ. To compare the model with tests, it is necessary to make the assumption that the *average* velocity over the area of the emergent jet corresponds to the *measured* velocity with which the jet leaves the screen as a growing geyser.[4]

The average velocity for normal impingement, derived by integrating over the range of r for which $\Delta P \geq 0$, namely, $0 \leq r \leq 2R_j$, is

$$V_{av} = \frac{\mu A}{6\rho}\left(\frac{\mu A}{\rho B V_j}\right)^2 \left\{\left[1 + \frac{2}{B}\left(\frac{\rho B V_j}{\mu A}\right)^2\right]^{3/2} - 1\right\} - \frac{\mu A}{2\rho B} \tag{7}$$

Calculations show that Eq. (7) overpredicts the test data of Ref. 4 by at least 100%. Reference 4 proposed a correlation for V_{av} which amounts to the use of 1/8 for an average C_P in Eq. (6), rather than the 1/4 arising implicitly from Eq. (7). Predictions from this correlation are within ±15% of the test data.[4] There is no apparent reason to explain a reduction of ΔP by a factor of 2; consequently, the correlation may not be reliable for other test data. In any case, it does not aid in understanding screen flows and so cannot be extended to other kinds of unconfined flows unless first verified by experimental data. The duct-flow model also overestimates test data for 45-deg impingement by about 100%.

Impinging Jet Screen-Flow Model

Since the duct-flow model does not give reliable predictions, a new or modified model is required. It seems likely that liquid flowing tangentially within the screen is the reason for the failure of the duct-flow model, which assumes a more or less straight-through path for the liquid. Liquid is deflected into the plane of the screen for all unconfined flows. The additional pressure drop caused by this increase in the flow-path length is not included in Eq. (1). There are several plausible ways, however, to incorporate the additional ΔP into a revised model. The basis of Eq. (1), namely, that the pressure drop is caused by a combination of viscous flow around the screen wires and inertial losses through parallel interconnecting channels between the wires, could be abandoned and the screen assumed to be a porous medium. Or the basic assumptions of Eq. (1) could be kept but the trajectory of the flow altered to account for the in-plane component.

For closely woven screens, it may be plausible to idealize a screen as a sort of porous medium that has a smaller internal resistance for flow in the plane of the screen than for flow across the thickness. Calculations[8] show that the in-plane resistance must be less than 1/1000 of the throughflow resistance to obtain correlation between test and theory. A flow resistance ratio of 1/1000 corresponds, roughly, to average pore diameters in the plane of the screen that are at least 30 times larger (for inertial losses) or 1000 times larger (for viscous losses) than the pores in the throughflow direction. These values seem too large to be reasonable. Thus, the porous medium model is probably not physically realistic.

Models that retain the basic assumptions of Eq. (1) can account for the nondirect flow path by increasing the factor Q, which is defined as the ratio of a typical path length to the screen thickness. The modified "tortuosity factor" can be estimated by assuming that the flow paths are inclined at an angle determined by both the throughflow velocity V and the effective tangential velocity V_s. As shown in Fig. 1b (for a twilled Dutch weave), the intercepted velocity is ϕV_s, where ϕ

‡The emerging jet has a velocity that is only a small fraction of the impinging velocity, and so the assumption of an impermeable screen is reasonable.

is a "blockage" coefficient depending on both screen and jet geometries, and V_s is the boundary-layer velocity at the screen upper surface. The velocity ϕV_s, combined with V, effectively selects a flow path inclined at the angle $\arctan(V/\phi V_s)$. The coefficient ϕ accounts for a number of factors: not all flow path angles are possible; the inclination of the path changes as the fluid passes through the screen, eventually being normal to the rear surface; and the screen weave is not axisymmetric about the stagnation point of the jet. It is further postulated that the intercepted velocity ϕV_s enters, exits, re-enters, re-exists, etc., the upper layer of wires as the flow is dragged along. Thus, the velocity passing through the screen is only the throughflow V and not the total velocity $(V^2+\phi^2 V_s^2)^{1/2}$ entering the upper surface; that is, the tangential velocity helps select a flow-tube inclination but does not otherwise affect the pressure drop. The flow-tube length is $l=bQ\,(V^2+\phi^2V_s^2)^{1/2}/V$, where Q is the tortuosity factor for duct flow. The relation between pressure drop and throughflow velocity for this model is

$$\Delta P = A\mu\sqrt{V^2+(\phi V_s)^2}+B\rho V\sqrt{V^2+(\phi V_s)^2} \tag{8}$$

Equation (8) makes mathematical sense only over a surface area for which the r coordinate is less than some $R_{max}\leq 2R_j$. The reason for this is neglect of the viscous shear at the screen surface, which has a component in the flow direction for large flow angles. Nonetheless, this model is valid over a large part of the impingement area, since numerical results to be cited later show that the throughflow in the region $r>R_{max}$ is negligible.

Boundary-layer velocities and thicknesses are estimated from results for a laminar unidirectional flow along a flat plate.[9] All of the tests of Ref. 4 had laminar boundary layers, but neglecting the radial divergence is an approximation, although the correct physical parameters are introduced. In any case, the empirical parameter ϕ can also account for the difference between radial and unidirectional flow. The boundary-layer thickness is $\delta=5\sqrt{\mu r/\rho V_r}$, which reduces to $\delta=6.97\sqrt{\mu R_j/\rho V_j}$ when Eq. (3) is used for V_r, or to $\delta=6.97\sqrt{\mu R_j/\rho V_j}\,(1+\frac{1}{2}\cos\theta)^{-1/2}$ when Eq. (5) is used. Since the screen penetrates into the boundary layer by about one-half a wire diameter ($b/6$ for a twilled Dutch weave), the effective surface velocity V_s is

$$V_s = 0.037(r/R_j)\sqrt{\rho b^2 V_j/\mu R_j} \tag{9}$$

This expression has been derived by the linearized approximation $V_s=(b/6)\,(dV_{BL}/dz)$ for $z=0$, where V_{BL} is the laminar boundary-layer velocity profile.[9] The numerical constant 0.037 is retained to get the correct order of magnitude for ϕ, which should be between zero and one. (Only the quantity ϕV_s enters the modeling expressions, and so the pure number 0.037 could, in principle, be absorbed into ϕ.) Equation (9) has been derived for a twilled Dutch weave but is valid within a factor of 2 for other weaves; this extra factor can be absorbed into ϕ.

Equations (8) and (9), together with the impingement pressure expressions, form the proposed mathematical model relating the emergent velocity to the impinging jet characteristics.

Solution for Emergent Velocity

Equation (8) must be averaged over the emerging jet area to predict the average throughflow velocity V_{av}. This averaging cannot be done exactly by analytical techniques. It is inconvenient to use numerical integration, since a value of ϕ must first be assigned, so an approximate analytical method has been used.[8] For normal impingement, the result is

$$\frac{V_{av}}{V_j}=\frac{1}{4\pi_1}\left\{\tfrac{1}{2}+\pi_2+2(\phi\pi_3)^2[2+2(\phi\pi_3)^2+\pi_2]+4(\phi\pi_3)^2[1+(\phi\pi_3)^2]\ln\frac{\phi\pi_3}{\sqrt{1+(\phi\pi_3)^2}}-2\phi\pi_3[2(\phi\pi_3)^2+\pi_2]\sqrt{1+(\phi\pi_3)^2}+\pi_2^2\ln\left[\frac{\pi_2+2\phi\pi_3[\sqrt{1+(\phi\pi_3)^2}-\phi\pi_3]}{\pi_2+1}\right]\right\} \tag{10}$$

Table 1 Values of blockage constant ϕ for twilled Dutch screens

Screen	Test liquid	Impingement velocity V_j, cm/s	Impingement angle, deg	Emergent velocity V, cm/s	Blockage constant ϕ	Predicted emergent velocity, cm/s
200×600	Ethanol	269	90	9.9	0.70	8.0
	Ethanol	226	90	6.2	0.70	5.6
	TCTFE[a]	194	90	12.9	0.70	14.4
	TCTFE	156	90	7.9	0.70	9.5
	TCTFE	125	90	3.7	0.70	6.1
	Ethanol	415	45	23.5	0.35	25.7
	Ethanol	380	45	22.0	0.35	15.8
	Ethanol	345	45	10.0	0.35	6.2
	Ethanol	315	45	5.6	0.35	0.1
	Ethanol	281	45	4.0	0.35	...
	TCTFE	200	45	19.9	0.35	33.6
	TCTFE	185	45	12.7	0.35	26.5
165×800	Ethanol	286	90	9.0	0.32	9.2
	TCTFE	170	90	10.8	0.32	10.6
	Ethanol	421	45	24.6	0.27	15.5
	Ethanol	411	45	21.1	0.27	15.0
	Ethanol	281	45	6.3	0.27	...
	TCTFE	184	45	10.9	0.27	18.0
	TCTFE	165	45	6.2	0.27	13.5
	TCTFE	141	45	6.0	0.27	8.5
80×700	Ethanol	362	90	7.1	0.18	6.6
	Ethanol	330	90	6.3	0.18	5.4
	TCTFE	210	90	6.4	0.18	7.5
	TCTFE	315	45	13.2	0.175	16.9
	TCTFE	275	45	10.9	0.175	10.9
	TCTFE	250	45	9.9	0.175	7.6

[a] TCTFE = trichlorotrifluoroethane.

Table 2 Screen parameters

	Twilled Dutch screens[a]			Plain[b] square screen
	165 × 800	200 × 600	80 × 700	400 × 400
Viscous resistance coefficient α	3.3	6.9	5.19	8.61
Inertial resistance coefficient β	0.17	0.3	0.2	0.52
Screen thickness b, cm	0.01753	0.015	0.0254	0.00509
Screen-volume void fraction ϵ	0.426	0.562	0.369	0.706
Screen pore diameter D, cm	0.0025	0.00399	0.0025	0.0038
Ratio of surface area to unit volume a, cm^{-1}	413.6	356	318	514
Tortuosity factor Q	1.3	1.3	1.3	1.0
Overall screen constants				
A, cm^{-1}	70,889	53,990	127,276	23,229
B	8.54	4.64	19.4	1.40

[a] Data from Ref. 4.
[b] Data from Ref. 1.

Table 3 Fluid properties at 20°C

	Liquid	
	Ethanol	TCTFE
Density ρ, g/cm^3	0.789	1.579
Viscosity μ, g/cm-s	0.012	0.007

and, for oblique impingement at 45 deg,

$$\frac{V_{av}}{V_j} = \frac{1}{4\pi_1}\left\{0.81+\frac{5}{2}\pi_2-6.79(\phi\pi_2)^3-2\pi_2^2\ell n\left(\frac{\pi_2+1}{\pi_2}\right)\right.$$
$$-\frac{4}{3}\pi_2^2\ell n\left(\frac{4\pi_2+3}{4\pi_2}\right)+(\phi\pi_3)^2[2+2(\phi\pi_3)^2+\pi_2]$$
$$+2(\phi\pi_3)^2[1+(\phi\pi_3)^2]\ell n\frac{\phi\pi_3}{\sqrt{1+(\phi\pi_3)^2}}$$
$$-(\phi\pi_3)[2(\phi\pi_3)^2+\pi_2]\sqrt{1+(\phi\pi_3)^2}$$
$$\left.+\frac{\pi_2^2}{2}\ell n\left[\frac{\pi_2+2\phi\pi_3[\sqrt{1+(\phi\pi_3)^2}-\phi\pi_3]}{\pi_2+1}\right]\right\} \quad (11)$$

With respect to exact integration, Eq. (11) is less accurate than Eq. (10).

The impingement area over which the model for normal impingement yields physically real effects (e.g., $V>0$ when $\Delta P>0$) is

$$r \le R_{max} = 2R_j[\sqrt{1+(\phi\pi_3)^2}-\phi\pi_3] \quad (12)$$

A similar but more complicated expression can be derived for oblique impingement.

The degree to which the mathematical model of the throughflow represents reality can be inferred from comparison with test data. A "good" comparison requires that 1) a single value of ϕ between zero and one correlates all test data for a given screen weave and impingement angle, regardless of fluid properties or jet velocities and diameters; and 2) R_{max} be not too much smaller than $2R_j$. If these requirements are met, then it can be reasonably concluded that the proposed model does incorporate all the important physics of the flow, is valid, and can be used reliably to predict throughflows.

Results and Discussion

Substantial amounts of data are available from experiments conducted at NASA Lewis Research Center (Ref. 4 and high-speed 16-mm motion pictures for unreported tests). At relatively high test velocities, liquid continually penetrated the screen to form a growing geyser. The steady-state throughflow measured in these tests constitutes the data used to verify the proposed screen-flow model.

Verification of Model

Twilled Dutch Screens

NASA test results for normal and oblique impingement are shown in Table 1. Two other screens (325 × 2300 and 200 × 1400) were used, but throughflow was not observed for the tested conditions. Geometrical constants for the screens and physical properties of the fluids are given in Tables 2 and 3. All impinging jets had diameters of 0.625 cm.

For a given screen and test conditions, Eq. (10) or Eq. (11) was used to predict the average throughflow velocity as a function of the blockage coefficient ϕ. Typical results are shown in Fig. 2. As ϕ increases, the throughflow decreases, which is the desired behavior. The range of ϕ values needed to correlate the data is fairly small, regardless of liquid properties or jet velocities, thus tending to validate the model. (The only exception is TCTFE test $V_j = 125$ cm/s; $\phi = 1.1$ is required to predict the throughflow velocity of this test. The correlation proposed in Ref. 4 also overpredicts this test point, by about 100%. It is believed that this data point is in error.) For this screen, at least, the best correlation of ϕ considering only TCTFE is slightly greater than the best correlation when only ethanol is considered. One of the premises of the model is that ϕ should not depend on fluid properties. The observed discrepancies are not large enough to invalidate this premise.

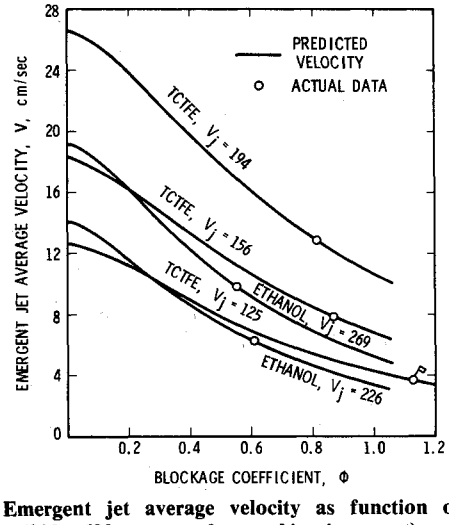

Fig. 2 Emergent jet average velocity as function of blockage coefficient (200 × 600 screen and normal impingement).

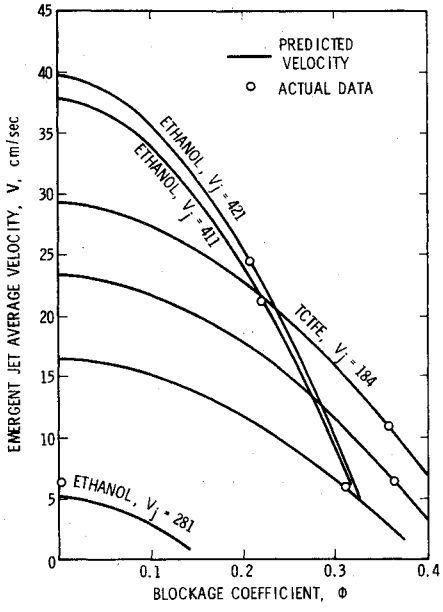

Fig. 3 Emergent jet average velocity as function of blockage coefficient (165 × 800 screen, 45-deg impingement).

Typical results for oblique impingement are shown in Fig. 3. There is more scatter in the value of ϕ needed to predict each test than there is for normal impingement. At least two causes contribute to this. First, the mathematical model is less exact because of the approximate pressure distribution used and the number of mathematical approximations need to derive Eq. (11). Second, twilled Dutch screens have different geometrical properties in different lateral directions, but not all the tests were conducted with the same orientation of the screen weave to the inclined-jet axis. TCTFE data again seem to be correlated by larger values of ϕ than ethanol.§ The model fails to predict the ethanol test $V_j = 281$ cm/s. In fact, even $\phi = 0$, which corresponds to Eq. (1), underpredicts the test slightly. Consequently, it is neglected in determining the best correlating value of ϕ. An analogous situation (i.e., the best value of ϕ being much smaller for one test of a group) occurred for the 200 × 600 screens with ethanol and $V_j = 281$ cm/s. Both of these tests had little throughflow, and so the velocities are subject to relatively large measurement errors.

The overall best correlations for ϕ are shown in Table 1. Predicted values of V_{av} using these values of ϕ are also given, except for the two cases of small throughflow mentioned previously for which the model seems to fail. Several conclusions are evident. Blockage constants for a given screen are larger for normal than for oblique impingement. Furthermore, the correlation between the measured and predicted emergent-jet velocity is better for normal than for oblique impingement as a result of the smaller variation in the best ϕ from one test to another for normal impingement.

The largest value of $\phi\pi_3$ is 0.52, corresponding to the 80 × 700 screen and the smallest ethanol jet velocity. From Eq. (12), $R_{max} = 1.25\, R_j$ for $\phi\pi_3 = 0.52$. For the bulk of the tests, a value of $\phi\pi_3 \approx 0.35$ is more appropriate, and so the model is mathematically valid over most of the impingement area for most of the tests.

The overall quality of the normal impingement correlation is shown in Figs. 4 and 5. Comparisons of predicted and measured velocities are about as good as that shown in Ref. 1 as the basis for Eq. (1).

Plain Square Screens

Two normal-impingement tests using a 400 × 400 plain square weave screen were also compared to the model. The

§Not all screens exhibited this behavior.

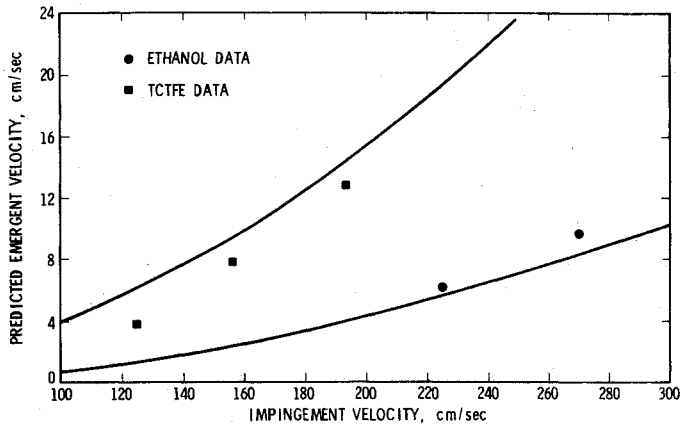

Fig. 4 Comparison of data and model using best correlation for blockage coefficient (200 × 600 screen, normal impingement).

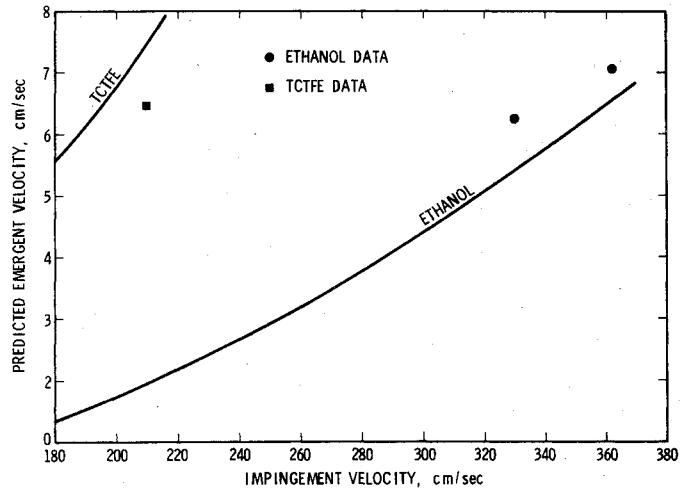

Fig. 5 Comparison of data and model using best correlation for blockage coefficient (80 × 700 screen, normal impingement).

predicted values for $\phi = 0$ are close to the test results, as might be expected because of the open weave of these screens. For $V_j = 214$ cm/s, the predicted value from Eq. (10) with $\phi = 0$ is 28.4 cm/s as compared to the test value of 26.5 cm/s; and for $V_j = 246$ cm/s, the prediction is 36.3 cm/s as compared to the test value of 30.3 cm/s. For open screens, the concept of a blockage coefficient has little meaning, and in fact the predicted throughflow velocity decreases by only 10% over a range of ϕ from zero to one. In making the predictions, the general values of $\alpha = 8.61$ and $\beta = 0.52$[1] were used, since specific data for a 400 × 400 screen are not available. Considering the spread of the data shown in Ref. 1, the agreement between test and model predictions for $\phi = 0$ is very good.

Percentage of Liquid Passing through the Screen

The total flow rate through the screen can be calculated by multiplying the average throughflow velocity by the cross-sectional area of the emergent jet. For normal impingement, the emergent area is four times the impingement area, or $4\pi R_j^2$. For impingement at 45 deg, the area as calculated from the equation of the emergent jet periphery, $r = R_j\,(2 + \cos\theta)$, is $4.5\,\pi R_j^2$.

Conclusions

Physical and mathematical models have been proposed for an unconfined flow impinging upon a fine-mesh screen. The starting point of the model is the relation between throughflow velocity and pressure drop previously developed for duct flow across a screen. It has been modified to account for the

increase in flow-path length through the screen which results from the deflection of the unconfined flow. Detailed mathematical results were presented for a circulat jet impinging either normally or obliquely (at 45 deg) on a screen. One important consequence of the model is that a new parameter, the blockage coefficient, is required to model the impingement flow accurately. Empirical values of te blockage coefficient were determined by comparison with test data from previous studies.

The following conclusions were drawn:

1) The model verifies the experimental result that the emerging diameter is about twice as large as the impinging diameter.

2) Blockage coefficients depend only on screen geometry and jet impingement angle. Coefficients for normal impingement are somewhat larger than for oblique impingement.

3) The proposed model correlates normal impingement results more accurately than oblique impingement results. This is probably not a basic shortcoming of the model, but a result of approximations made in the mathematical development and scatter in the oblique-impingement data. Predicted velocities for normal impingement, using the recommended correlation of the blockage coefficient for each screen, generally agree within $\pm 15\%$ with tests.

It is clear that further tests are needed to define blockage coefficients for other screens and to validate more completely the proposed throughflow model.

Acknowledgment

This research was sponsored by NASA Lewis Research Center, Contract NAS3-20086. E. P. Symons served as the NASA Technical Monitor and contributed several valuable suggestions.

References

[1] Armour, J. C. and Cannon, J. N., "Fluid Flow Through Woven Screens," *American Institute of Chemical Engineers Journal*, Vol. 14, May 1968, pp. 415-420.

[2] Cady, E. C., "Study of Thermodynamic Vent and Screen Baffle Integration for Orbital Storage and Transfer of Liquid Hydrogen," McDonnell-Douglas Astronautics Co., MDC-G4798, Contract NAS3-15846, NASA CR-134482, 1973.

[3] Blatt, M. H., Start, J. A., and Siden, L. E., "Low Gravity Propellant Control Using Capillary Devices in Large Scale Cryogenic Vehicles," General Dynamics/Convair, Design Handbook, GDC-DDB70-006, Contract NAS8-21465, Aug. 1970.

[4] Symons, E. P., "Normal Impingement of a Circular Liquid Jet Onto a Screen in a Weightless Environment," NASA TM X-3415, Aug. 1976.

[5] Bernardi, R. T., Lineham, J. H., and Hamilton, L. H., "Low Reynolds Number Loss Coefficients for Fine-Mesh Screens," *Journal of Fluids Engineering*, Vol. 98, Dec. 1976, pp. 762-763.

[6] Schach, W., "Umlenkung eines kreisförmigen Flüssigkeitsstrahles an einer ebenen Platen senkrecht zur Strömungsrichtung," *Ingenieur-Archiv*, Vol. 6, No. 1, 1935, pp. 51-59 (transl. provided by NASA Lewis Research Center).

[7] Schach, W., "Unlenkung eines freien Flüssigkeitsstrahles an einer ebenen Platte," *Ingenieur-Archiv*, Vol. 5, No. 4, 1934, pp. 245-265; also NASA TT F-15, 1973.

[8] Dodge, F. T. and Ricker, R. E., "Study of Liquid Jet Impingement on Screens," Southwest Research Inst., Final Rept. 02-4492, Contract NAS3-20086, NASA CR-135260, Sept. 1976.

[9] Schlichling, H., *Boundary Layer Theory*, 4th Ed., McGraw-Hill, New York, 1960.